Abnormal Basal-Body Number, Location, and Orientation in a Striated Fiber-defective Mutant of *Chlamydomonas reinhardtii*

ROBIN L. WRIGHT, BONNIE CHOJNACKI, and JONATHAN W. JARVIK
Department of Biological Sciences, Carnegie-Mellon University, Pittsburgh, Pennsylvania 15213

ABSTRACT We describe a mutant of *Chlamydomonas reinhardtii* in which basal body associated striated fibers are absent or incomplete. Basal body spacing, angle, and relative rotational orientation are abnormal and extremely variable. Abnormal partitioning of cellular contents at cytokinesis is also evident. Mating, maintenance of flagellar length equality, and backward swimming response are normal. Genetic analysis indicates mutation of a new Mendelian gene—*vfl-3*—linked to the centromere of Chromosome VI.

Striated fibers associated with basal bodies (6, 26, 30, 44) and centrioles (21, 34, 39) have been observed in numerous eucaryotic cells, and they have been given a variety of names, including rhizoplasts (8), kinetodesmal fibers (1), and ciliary or flagellar rootlets (20). The association of striated fibers with basal bodies and centrioles is so characteristic that a relationship among all striated fibers—or at least the existence of a limited number of fiber families—seems probable (5, 26), in spite of the considerable variation in size, shape, and periodicity shown by fibers from different sources.

The very ubiquity of striated fibers makes it likely that they play important cellular roles. A number of passive roles such as anchoring or supporting basal bodies, maintaining basal body position or dissipating mechanical stress have been proposed for the fibers (30, 44). More active roles have also been considered. For instance, it has been suggested that the fibers coordinate motility, since when basal bodies are linked by striated fibers their flagella typically show coordinated beating (3, 7, 12, 15). Observations of ATPase activity in fiber cross-bands (2, 24), proximity between mitochondria and striated fibers (28, 40, 42), and variations in fiber periodicity (14, 35, 36) have all been cited as suggesting an active contractile function for the striated fibers (30, 37). Salisbury and Floyd (35) demonstrated calcium-dependent contraction of a large striated fiber—the rhizoplast of *Tetraselmis*—and they were able to produce cycles of contraction/relaxation by alternate incubations with and without $CaCl_2$ and ATP. A calcium-dependent decrease in the normal 90° angle between the paired basal bodies of isolated *Chlamydomonas* flagellar apparatuses was reported by Hyams and Borisy (15), who speculated that this might be due to striated fiber contraction.

We decided to approach the question of striated fiber function by isolating and examining fiber-defective mutants in the biflagellate alga *Chlamydomonas reinhardtii*. The two basal bodies of *C. reinhardtii* are oriented at right angles to one another and are connected by three striated fibers (32). The largest of these, the "distal striated fiber," connects the basal bodies near their cell-distal ends. The distal fiber has approximate dimensions of 300 nm × 250 nm × 75 nm and a banding pattern consisting of a central pair of dark striations flanked on either side by two light bands, two dark bands, and a dark band close to the basal body (see Fig. 2*b*). Two parallel "proximal striated fibers" connect the basal bodies at their cell-proximal ends. Proximal fibers have approximate dimensions of 140 nm × 45 nm, and each carries three or four cross striations (see Fig. 2*c*).

Having reasoned that striated fibers are probably necessary for normal coordination of flagellar motility, we isolated a number of aberrant motility mutants and examined them for striated fiber defects. Here we describe the phenotype and ultrastructure of a mutant clearly defective with respect to its striated fibers.

MATERIALS AND METHODS

Strains and Culture Conditions: Wild-type strains used were the 137c derivatives *NOmt*$^+$ and *NOmt*$^-$ provided by Dr. U. Goodenough (Washington University). Strains CC530 (*ac17mt*$^-$), CC 624 (*pf16mt*$^-$), CC1084 (*nr-1thi-1mt*$^+$) and CC1139 (*nr-1thi-1mt*$^-$) were provided by the Chlamydomonas Genetics Center, Duke University (Durham, NC). *vfl-2* was *vfl-2-220* (19). Cells were grown at 25°C in medium I of Sager and Granick (33), bubbled continuously with filtered air. Cultures were illuminated with white light (45 cm from two General Electric F48T12-CW-HO fluorescent tubes; General Electric Co., Wilmington, MA) and synchronized by a 14 h light/10 h dark cycle. Experiments were typically performed between hours 2 and 6 of the light segment of the cycle.

Mutagenesis and Mutant Isolation: Log phase *NOmt*$^+$ cells were spread on 1.5% agar plates and exposed to ultraviolet light (48 cm from a General Electric Co. G30T8 germicidal lamp) for 90 s (16, 23). Cell survival was

~40%. Plates were stored in the dark for 4 h to prevent photoreactivation and then incubated in constant light at 25°C until colonies were clearly visible to the naked eye. Individual colonies were picked from the plates into capillary tubes containing liquid media and subsequently scored for motility under a dissecting scope at × 80. Strains with motility defects (immotile, slow, or aberrant) were retained and examined under phase optics (× 800) to verify and further characterize their mutant phenotypes.

Measurements of Flagellar, Location, and Length: Cells were fixed by addition of ½ volume of 1% aqueous glutaraldehyde, and phase-contrast microscopy at × 800 was used to score number and location of flagella. Flagellar length was measured with an ocular micrometer, using the same optics. Distribution of flagella in a population was based on scoring no less than 200 cells per sample. Average values for flagellar length were determined from measurements of 20 or more cells of each flagella-number class, unless otherwise noted.

Motility Observations: Observation of living cells used phase-contrast microscopy at magnifications between 125 and 800. Flagella of live *C. reinhardtii* often become momentarily attached to the glass slide or coverslip; by counting the number of flagella on a cell when the flagella were attached and by observing motility after the cell detached, correlation between flagella number and cell motility could be made.

Electron Microscopy: Cells between the second and fourth hours of the light segment of the illumination schedule were harvested by gentle centrifugation (5 min at 2,500 rpm in a Beckman TJ-6 centrifuge, Beckman Instruments, Inc., Palo Alto, CA) in glass culture tubes and then subjected to either of the following fixation protocols.

COLLIDINE-BASED FIXATION: To the pellet of cells, ½ ml of an ice-cold solution composed of 2.5% glutaraldehyde, 0.2% tannic acid, and 0.1 M S-collidine, pH 7.8, was added. The pellet was resuspended in the fixative, then repelleted as described above. The initial fixation solution was removed and fresh fixative added carefully to avoid disturbing the pellet. (Centrifugation was repeated throughout the protocol, as required, to maintain the pellet.) Fixation was allowed to proceed, on ice, for 1 h. Cells were then rinsed with at least five changes of ice-cold 0.1 M S-collidine buffer, pH 7.8, over a period of at least 1 h, keeping cells on ice. At this point, samples were often stored at 4°C overnight. Samples were postfixed for 1 ½ to 2 h in ice-cold 1% osmium tetroxide in 0.1 M S-collidine buffer, pH 7.8, rinsed twice in water, and stained en bloc with 1% aqueous uranyl acetate for 15–20 min.

CACODYLATE-BASED FIXATION: To the pellet of cells we added 0.5 ml of an ice-cold freshly prepared solution of 2.5% glutaraldehyde, 2% OsO_4 in 0.1 M sodium cacodylate buffer, pH 7.8. The pellet was resuspended in the fixative and allowed to stand on ice for 5 min. The cells were repelleted and the initial fixative was replaced with an equal volume of fresh fixative. After 30 min, we washed samples at least five times in 0.1 M sodium cacodylate buffer, pH 7.8. Samples could be stored overnight at 4°C in buffer at this point. Pellets were postfixed with 2% OsO_4 in 0.1 M sodium cacodylate, pH 7.8, for 1.5–2 h and rinsed two times in water. If en bloc staining was to be performed, we also rinsed the sample twice with 50% aqueous ethanol. En bloc staining was accomplished with 0.25 to 0.5% aqueous uranyl acetate for 15 min.

All samples were rapidly dehydrated in a graded alcohol series, followed by two rinses in propylene oxide, and infiltrated with resin (60 ml of DDSA, 20 ml of Araldite 502, 20 ml of Embed 812, and 3 ml of DMP-30). Infiltration was facilitated by use of a vacuum oven (50°C, 10 lbs psi). The resin was polymerized at 60°C for 12 to 48 h. Silver-to-gold sections were cut with a glass or diamond knife on an MT-1 or MT-2 microtome. Sections were stained with 3% uranyl acetate and Reynold's lead citrate (31) and examined with a Philips 300 electron microscope.

The collidine-based fixation protocol produced good preservation of the basal body region but less than adequate fixation of the nuclear membrane, Golgi, eye-spot, and mitochondria. The cacodylate-based protocol appears to give excellent preservation of all cytoplasmic, membranous, and extracellular structures.

Mitotic Pedigree Analysis: At about the eight hour of light cycle, cells were suspended in melted agarose (final agarose concentration = 0.07%). A drop of this suspension was placed within a ring of petroleum jelly on a glass slide and sealed with a coverslip. Cell positions were recorded with the vernier scales on the stage control of the microscope, and flagellar number was noted. The slides were maintained overnight on the original light/dark cycle, during which time one or more rounds of mitosis occurred. The next morning flagellar number on each daughter cell was recorded.

Genetic Analysis: We used standard methods for gametogenesis (18), mating, and tetrad dissection (22). Centromere linkage was determined using the centromere-linked marker *ac17* and applying the relation 1/2T / PD+NPD+T. Marker-marker distance for linked markers was calculated using the relation T+6NPD / 2(PD+NPD+T) (29).

RESULTS

Isolation of vfl-3

In a screening of 2037 mutagenized clones, we identified 33 aberrant swimming mutants. Among the initial five that we examined by thin-section electron microscopy to determine striated fiber phenotype, one (RW207) was found to present distinct fiber defects. Genetic analysis (see below) revealed that RW207 carries a mutation in a previously unidentified mendelian gene. We have given this gene the name *vfl-3* (for variable flagellar number), and the allele the name *vfl-3-207*. As this is the only *vfl-3* allele identified to date, we will refer to it simply as *vfl-3* throughout this paper.

Distribution, Location, and Length of Flagella in RW207

Variable number of flagella per cell is a striking feature of the *vfl-3* phenotype. As indicated in Table I, roughly equal numbers of cells with zero, one, and two flagella comprise ~90% of a mutant population; cells with three or four flagella are not uncommon, and at low frequency (<0.3%) cells with five or more flagella are present. Flagellar number per cell averages 1.3.

In addition to flagellar number defects, many *vfl-3* cells show abnormalities in the sites of flagellar placement on the cell surface. In ~10% of the cells, flagella are located offcenter or to the side, whereas in wild-type controls they are found exclusively at the anterior cell apex. Such flagellar displacements are more likely to occur on cells with two or more flagella. Distinct pairing of the flagella is commonly observed on cells with two or more flagella, so that many cells can be scored as having one pair plus one single, two pairs, etc. Average flagellar length is 9.8 μm, about 2 μm shorter than wild-type controls. With increased flagellar number, average flagellar length decreases (Table I), but the effect is not dramatic. As in wild-type biflagellates, all flagella on individual multiflagellate *vfl-3* cells are equal in length.

Mitotic Pedigree Analysis

A *pf16,vfl-3* double mutant was constructed and used in mitotic pedigree analysis. The *pf16* mutation renders cells immotile, so that daughters of individual cells can easily be scored for flagellar number before and after division. The results indicate no close relationship between flagellar number of a parent cell and flagellar number of its progeny. We frequently observed abnormally small daughters among the progeny of individual *vfl-3* cells, and cell debris was present in

TABLE I

Frequency Distribution of Flagellar Number Classes in vfl-3

No. of flagella/cell	% Total cells scored*	Average flagellar length‡
		μm
0	20	—
1	36	10.8
2	34	9.8
3	7.5	9.5
4	1.7	8.5

* 2,061 cells scored.

‡ Average of 45 or more cells, except for quadriflagellate class, which is the average of 11 cells.

the mutant microcolonies in many cases. Furthermore, many mutant microcolonies contained odd numbers of cells, whereas most control (*pf-16*) microcolonies contained either four or eight cells. The death and lysis of some daughters, and the abnormally small size of others, suggest a defect in the control of cell division.

Light Microscopic Observations—Motility

Vfl-3 cells display a diverse and complex motility pattern. The majority of motile cells rotate in place. Monoflagellates show this kind of twirling motility, but, surprisingly, most biflagellates show twirling behavior as well. A "motile twirl" pattern is displayed by some biflagellate cells; these cells twirl as described above, but they also progress slowly across the field of view, looking like spinning tops. In addition to the predominant twirlers, cells with a wide variety of other abnormal patterns are present. Wildly erratic motility, zig-zagging, flagella-first tumbling, and slow swimming are all observed in mutant cultures. Very rare cells swim in a pattern approaching normal, but truly wild-type motility has not been observed.

In *Chlamydomonas* a sudden increase in illumination or collision with an object produces a backward-swimming response: flagella are thrown forward, the beat pattern changes from a ciliary to a flagellar (i.e., symmetric) form, and the cell moves slowly backward. A normal backward-swimming response has been observed in mutant cells of all motility types, regardless of number of flagella.

Vfl-3 cells are not generally capable of phototaxis. Thus cells in cultures illuminated from above do not gather at the meniscus as wild-type cells do; rather, they fall to the bottom of the culture vessel. The absence of phototactic ability in mutant cells is probably a consequence of their grossly aberrant motility, and we believe that it does not reflect a primary defect in phototaxis itself. A few cells (<6%) make it to the surface, and observation of these cells indicates a pronounced enrichment for the less severely affected motility types such as tumblers and slow-swimmers.

Light Microscopic Observations—Fixed Cells

Observation of glutaraldehyde-fixed cells indicates a clear defect in flagellar spatial coordination in *vfl-3*. Fig. 1 shows tracings of a number of randomly chosen mutant and wild-type cells. The 180° rotational symmetry characteristic of the two wild-type flagellar wave forms is clearly not characteristic of mutant biflagellates since, in about half the cases, both of their flagella bend in the same direction. Temporal coordination in the mutant is more difficult to assess. Having followed many flagellar wave forms in three dimensions using Nomarski differential interference contrast optics, we get the impression that all flagella on individual mutant cells are very nearly in phase with one another. However, because glutaraldehyde fixation is not truly instant, we prefer to await direct cinematic or video observation of live mutant cells before reaching firm conclusions about temporal coordination.

Defective Basal-Body Orientation and Position in vfl-3

Basal body, transition region, and axoneme structure in *vfl-3* are generally normal, as the thin-section electron micrographs in Fig. 2 illustrate. However, striking abnormalities in basal-body position and orientation are evident. Whereas wild-type control cells show little variation in angle and distance between their two basal bodies, we observed wide variation in the mutant. Results of measurements made on micrographs containing longitudinal sections through two or more basal bodies are tabulated in Table II. Note that the majority of mutant pairs have angles <60°, whereas we observed no angle <62° in wild type. In wild-type cells, measured distances between the centers of transition regions exhibited only a limited range (600–770 nm), while the distance in mutant cells ranged widely (330–1,980 nm). Perfect longitudinal sections through both basal bodies are never seen in wild-type cells because the longitudinal axes of the two basal bodies lie in different planes, separated by slightly less than one basal-body

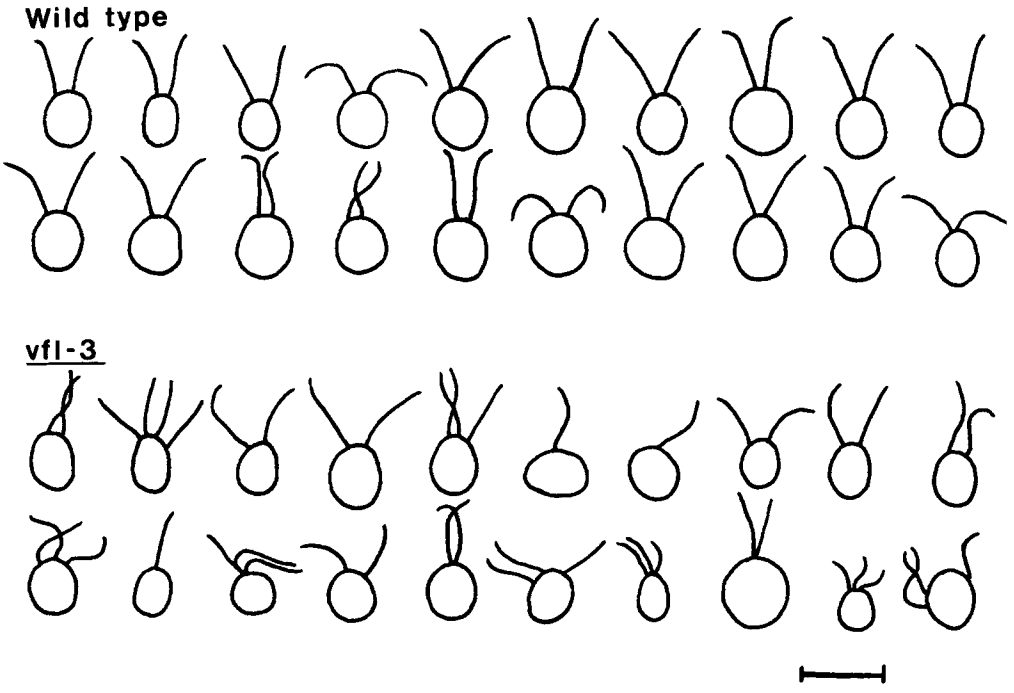

FIGURE 1 Tracings from differential interference-contrast photomicrographs of fixed wild-type and RW207 cells. Bar, 10 μm.

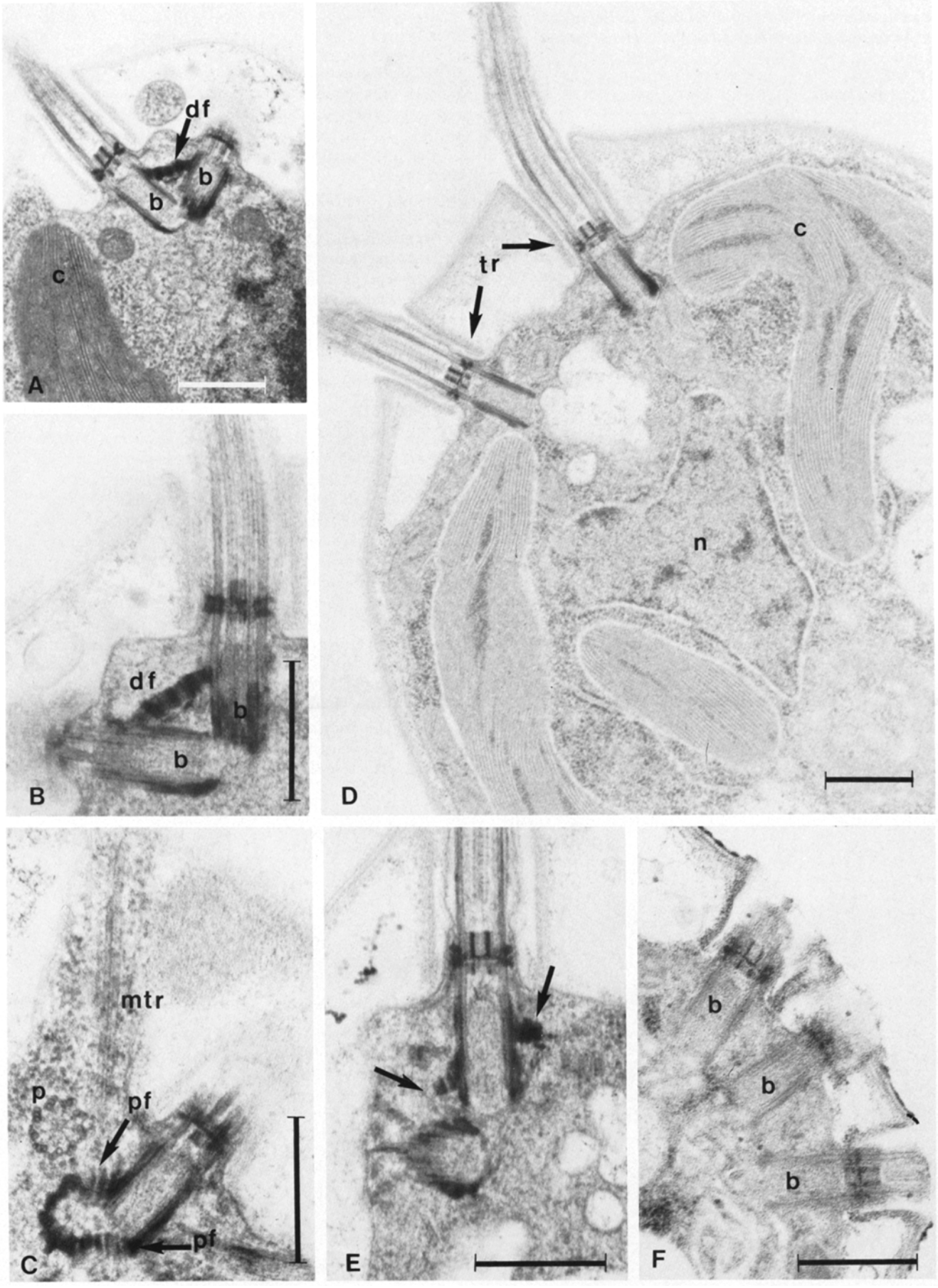
df
b
b
c
A
tr
c
n
D
df
b
b
B
mtr
p
pf
pf
C
E
b
b
b
F

diameter, but such sections, sometimes including three basal bodies, have been seen a number of times in *vfl-3* (e.g., Fig. 2 *d* and *f*). It is our clear impression that the number of basal bodies per *vfl-3* cell is considerably greater than in wild type even though the number of flagella per cell averages only 1.3; thus, mutant cells must contain many basal bodies without attached axonemes.

TABLE II

Inter-Basal-Body Angle and Distance in vfl-3 and Wild Type

NO^+ (wild type)		*vfl-3*	
Angle in degrees	Distance	Angle in degrees	Distance
	nm		*nm*
		9	360
62	720	19	1,140
67	600	59*	800*
71	630	24*	330*
73	650	35*	470*
76	660	25	720
77	680	35	960
84	720	35	1,170
86	770	38	480
87	710	44	660
89	690	45	630
90	680	55	1,980
90	770	60	680
		68	480
		95	560

* Triflagellate section.

A variety of arrangements are seen in sections showing three basal bodies. Observed arrangements include basal bodies approximately parallel and close together in the same plane, basal bodies approximately parallel and widely separated, and two basal bodies parallel, close together, and at a right angle to a third.

Abnormal flagellar location with respect to the cell as a whole is fairly common, with flagella extending from the sides of cells or from other abnormal positions. Basal bodies have been found deep in the cell interior rather than at the cell surface, and they can be parallel to the surface or even upside down (Fig. 3).

Striated Fiber and Microtubule Rootlet Defects in vfl-3

Mutant basal bodies are quantitatively deficient in striated fibers and when fibers are present they are incomplete, abnormal, and often improperly oriented. In spite of electron microscopic examination of thousands of thin-sections of *vfl-3* cells, no fully normal distal or proximal striated fibers (i.e., normal in terms of position, connectivity, and striation pattern) have

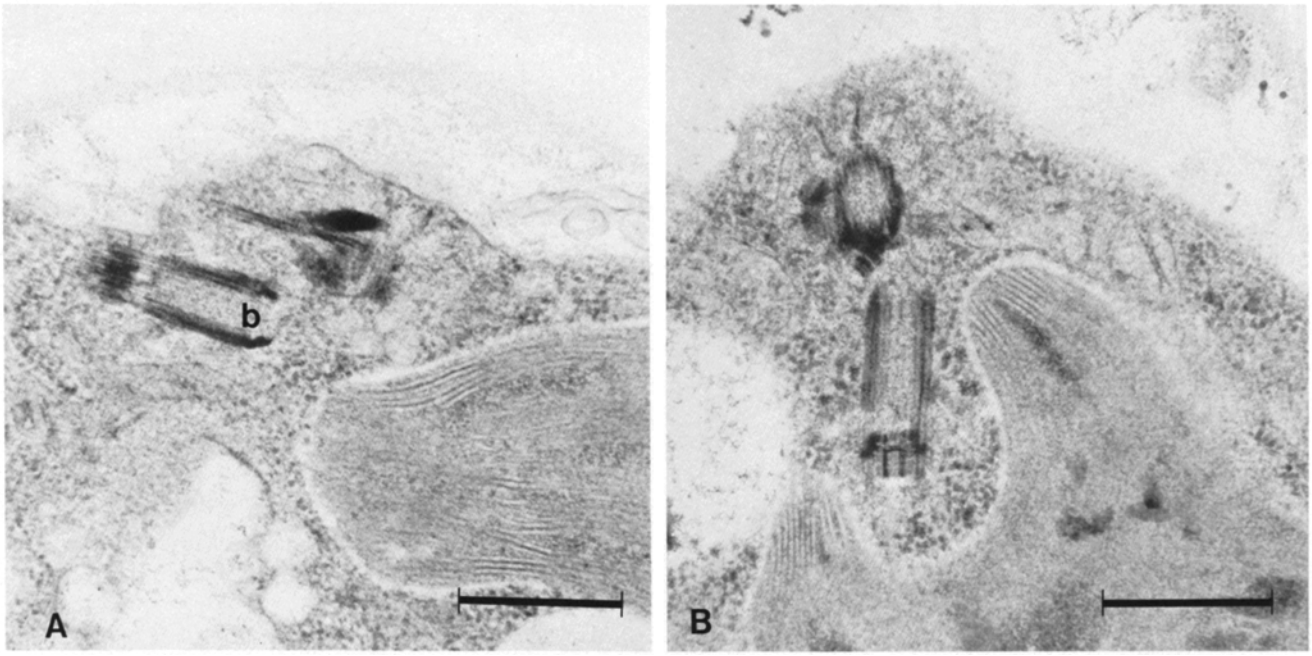

FIGURE 3 Abnormal basal-body placement in *vfl-3* cells (*A*) Basal body lying nearly parallel to cell surface. Collidine fixation. × 44,000. (*B*) Basal body upside down, with transition region facing cell interior. Note striated projection on other, transversely sectioned, basal body. Collidine fixation. Bar, 500 nm. × 44,000.

FIGURE 2 Relative placement of basal bodies in wild type (*A, B,* and *C*) and *vfl-3* (*D, E,* and *F*). (*A* and *B*) Wild type basal-body pairs, showing distal striated fiber. Collidine fixation. (*A*) × 33,000 and (*B*) 54,000. (*C*) Wild-type basal-body pair, showing proximal striated fibers. Note microtubular rootlets and probasal body. Collidine fixation. × 33,000. (*D*) Abnormal angle and spacing between *vfl-3* basal bodies. Note Absence of distal striated fiber. (*E*) Longitudinal section through *vfl-3* basal body, transition region, and axoneme. Basal-body structure appears fully wild type, but note abnormal projects from basal body (arrows). Collidine fixation. × 54,000. (*F*) Three *vfl-3* basal bodies in nearly perfect longitudinal section. Collidine fixation, × 45,000. (*b*) Basal body. (*c*) Chloroplast. (*df*) Distal fiber. (*mtr*) Microtubular rootlet. (*p*) Probasal body. (*pf*) Proximal fiber. (*tr*) Transition region. Bar, 500 nm.

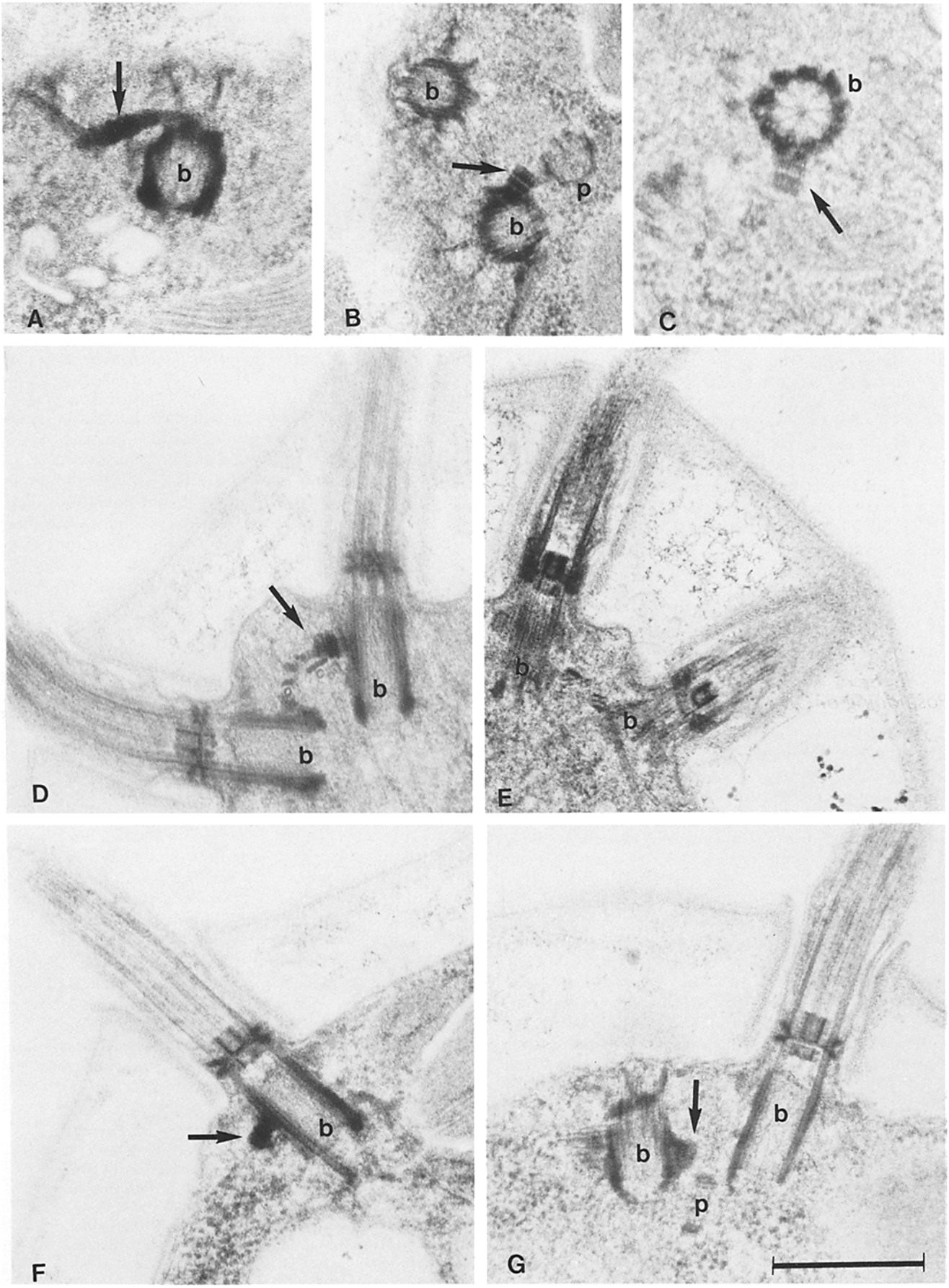
A
b
B
b
p
b
C
b
D
b
b
E
b
b
F
b
G
b
b
p

been observed. Mutant basal bodies may be completely free of fibers, or they may carry striated or non-striated projections at a variety of locations. Often, the projections have a diffuse and tenuous appearance as compared to wild-type striated fibers. With one exception, a projection has never been observed to fully span the space between the basal bodies, and even in this exceptional case fiber striations and basal body orientation were abnormal. Fig. 4 illustrates a variety of striated fiber defects observed in mutant cells.

Only 16% (19 of 116 basal bodies scored) of sections through mutant basal bodies showed evidence of attached projections or densities which resembled striated fibers, whereas 48% (71 of 147 basal bodies scored) of such sections in wild-type controls showed striated fibers of standard morphology. Because *vfl-3* cells contain extra basal bodies—i.e., basal bodies without attached axonemes—the high frequency of total fiberless basal bodies could reflect an abundant class of basal bodies with neither fibers nor axonemes.

In wild-type *Chlamydomonas*, four microtubular rootlets radiate into the cytoplasm from a dense plate (32) (also described as a "finely striated fiber" [10]) located between the basal bodies and beneath the distal striated fiber. Two of the rootlets typically consist of four microtubules which show a "3 over 1" arrangement as they approach the inter-basal body region, and the other two consist of a pair of microtubules each (10, 27, 32). In *vfl-3* the organization and positioning of the rootlet microtubules varies from cell to cell. The "3 over 1" configuration has not been observed, and in many cases microtubules are seen to extend through, rather than terminate at, the region between basal bodies. The dense plate is usually absent as well. Fig. 5 shows representative rootlet abnormalities in *vfl-3*, as well as patterns seen in wild-type controls.

Positioning of Other Organelles in vfl-3

Although the configuration of the entire basal-body complex is abnormal and highly varied in *vfl-3* cells, the overall orientation of other cellular organelles is usually normal. However, occasional displacements of the nucleus and/or pyrenoid occur, with the nucleus sometimes located far anterior near the basal bodies or with nucleus and pyrenoid side-by-side. Rare cells with two nuclei or pyrenoids have also been observed.

Genetic Analysis

Tetrad analysis of *vfl-3* is summarized in Table III. The mutation segregates 2:2 from wild type in tetrads derived from *vfl-3/wild-type* meioses. It is centromere-linked based on crosses against the centromere marker *ac17* (Table III, line 1). It is not linked to *nr-1* (Table III, line 2); since *nr-1* and the variable flagellar number mutation *vfl-1* (M. Adams, personal communication) are both on the right arm of Chromosome VIII, it follows that *vfl-3* and *vfl-1* are not linked. It is not linked to *vfl-2*, since of 32 *vfl-3* × *vfl-2* progeny examined eight were wild type (recombination frequency = 50%). Finally, we found that *vfl-3* is linked to the mating type locus (Table III, line 3), placing it on Chromosome VI. The calculated distance between *vfl-3* and *mating type* is 32 map units. This is fully consistent with *vfl-3's* centromere linkage, since *mt* and the centromere are about 35 map units apart. We conclude that the *vfl-3* mutation defines a new gene closely linked to the centromere of Chromosome VI.

DISCUSSION

Vfl-3 Defect Expressed Early in Basal-Body Cycle

In wild-type *Chlamydomonas* basal-body replication and segregation occur at characteristic points in the cell cycle. As early as 1 h after cell division two probasal bodies appear near the mature basal bodies (4) (Fig. 5*b*). Fibrous connectors join each probasal body to the mature basal bodies to form a basal body/ striated fiber/ probasal body complex which can be isolated intact from lysed cells (4, 11, 38). Elongation and maturation of the probasal bodies occurs during interphase, so that as cell division approaches four mature basal bodies are available for segregation to the two daughters.

Recent evidence suggests that basal-body segregation is semiconservative, with each daughter receiving one newly matured and one old basal body (13). Such a mode of segregation would clearly require that the striated fiber connections between the parental basal bodies be broken and that new connections between old and newly matured basal bodies be established. There are conflicting reports in the literature as to just when these events occur. Johnson and Porter (17) observed that cells in the midst of cytokinesis carry two pairs of basal bodies with the members of each pair connected by striated fibers—strongly suggesting that fiber dissolution and reappearance both precede cell division. In contrast, Cavalier-Smith (4) found that daughter cells shortly after cell division contained basal-body pairs which lacked striated fibers. The basal bodies were close together and nearly parallel (an arrangement reminiscent of what is frequently seen in *vfl-3*). Differences in strains or culture conditions could account for these discrepancies. We have not determined which pattern prevails in our cultures.

In *vfl-3* isolated probasal bodies unconnected to mature basal bodies or other probasal bodies are frequently observed by mid-interphase (e.g., Fig. 6*f*). We conclude that the *vfl-3* defect is expressed before this time—i.e., early in the cell cycle. Indeed, it is reasonable to propose that the host of ultrastructural defects observed in *vfl-3* all derive from a primary failure to properly position probasal bodies in the young cell, since without appropriate basal-body placement: (*a*) striated fibers might be unable to form properly, (*b*) microtubular rootlets might be unable to arrange themselves correctly, and (*c*) orderly basal-body segregation at cell division might be impossible.

FIGURE 4 Representative striated fiber abnormalities observed in *vfl-3* sections. (*A*) Dense projection at distal fiber level. The projection appears to contact a rootlet microtubule. (*B*) Striated projection extending from basal body towards a probasal body. The projection resembles a proximal fiber, but it is at distal fiber level. (*C*) Proximal end of basal body (indicated by cartwheel interior) with striated projection. (*D*) Nearly normal basal-body orientation, but incomplete distal fiber (arrow). Note abnormal placement of rootlet microtubules, one in the diffusely striated region and two beneath the fiber and near a dense plate. (*E*) No distal fiber is evident in this section. Equivalent sections of wild type always show the fiber. (*F*) A dense projection at distal fiber level. Note the overlength microtubule on the basal body. (*G*) Dense projection on obliquely sectioned basal body. (*b*) Basal body. (*p*) Probasal body. Collidine fixation. Bar, 500 nm. × 54,000.

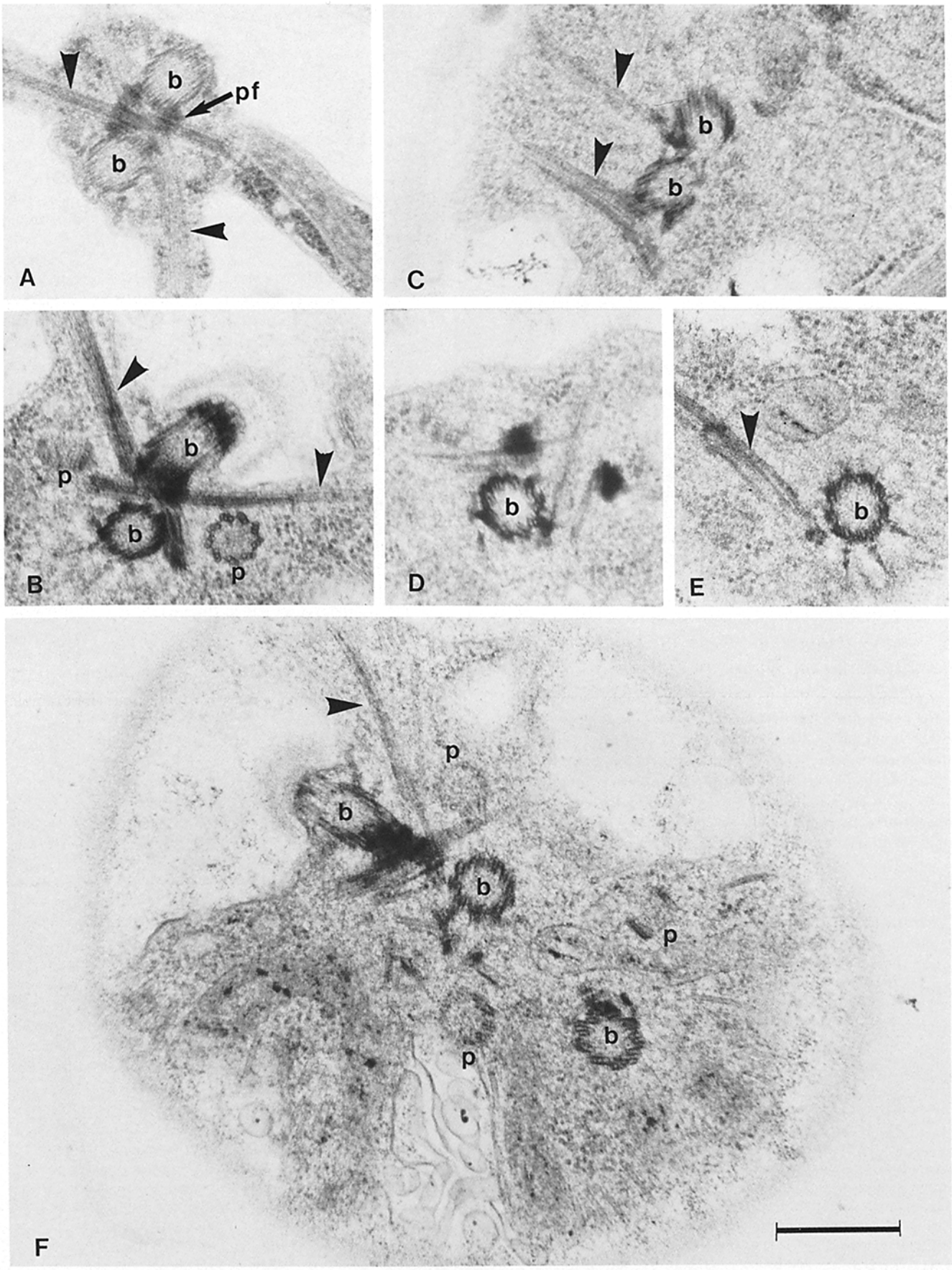
A
b
pf
b
C
b
b
B
b
p
b
p
D
b
E
b
F
p
b
b
p
b
p

TABLE III

Tetrad Analysis

Markers scored	PD	NPD	T
vfl-3, ac-17	5	8	0
vfl-3, nr-1	11	14	39
vfl-3, mt	36	1	51

The absence of a simple mitotic segregation pattern with respect to flagellar number is consistent with such unorderly segregation. However, because *vfl-3* appears to contain many basal bodies without attached flagella, it is not possible to unequivocally infer the pattern of basal-body segregation from the flagellar number data.

Generalized Somatic Segregation Defects in vfl-3

Vfl-3 cells appear to possess a defect in accurately partitioning their contents at cytokinesis. Cell size is highly variable as compared to wild type (Fig. 1), and individual cells have been directly observed to yield daughters of unequal size. Consistent with a cell division defect, a small but significant fraction of cells are binucleate or bipyranoidal. In light of the fact that the cleavage furrow in the dividing *C. reinhardtii* cell is lined with numerous microtubules which radiate from very near the basal bodies (17), we feel it likely that improper cleavage furrow positioning, and hence unequal partitioning of the cell's contents at division, represents a consequence of improper basal-body positioning.

Inferences about Basal-Body and Striated Fiber Polarity Based on Symmetry Considerations

Chlamydomonas flagella beat with the highly asymmetrical pattern typically exhibited by cilia. The two wave forms display a 180° rotational symmetry with respect to one another, resulting in a flagella-first swimming pattern. While the structural basis for flagellar beat asymmetry is not known, it is clear that in spite of its dominant ninefold rotational symmetry the flagellum has a number of elements which are not ninefold rotationally symmetric (43), and so it is safe to say that a structural polarity underlies the functional polarity expressed in the organelle's highly asymmetric beating.

Our results suggest the hypothesis that each basal body has an intrinsic polarity which determines the rotational orientation of the attached flagellum and hence the direction of the effective stroke. We reason as follows: the basal body shows ninefold rotational symmetry with respect to its major structural components, but is not ninefold symmetrical with respect to its striated fibers. If we hypothesize that the polarity associated with fiber attachment is determined by an intrinsic polarity in the basal body, and if we make two conservative assumptions—(*a*) that the two basal bodies are structurally identical, and (*b*) that the striated fiber attachment sites on each basal body are unique—it follows from symmetry considerations alone (see Fig. 6) that the two basal bodies are 180° rotationally symmetric (and thereby show the same rotational symmetry as the two flagellar wave forms).

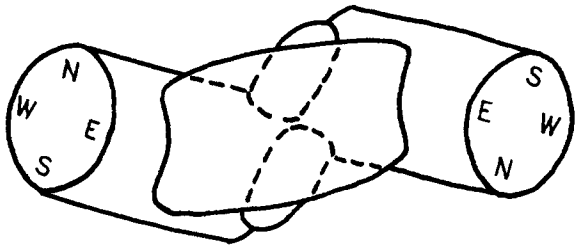

FIGURE 6 Cartoon view of basal body pair seen from above, showing the large distal fiber and the two smaller proximal fibers. Four radial coordinates—*N, S, E,* and *W* are included to emphasize the rotational symmetry.

Symmetry considerations lead to several additional speculations about striated fiber length, orientation, and banding patterns. First, it should be noted that the sites of distal fiber attachment are equivalent on the two basal bodies. Thus if fiber assembly can initiate on one basal body it ought to be able to initiate on the other as well. This leads us to propose a model wherein complete fibers arise by the joining of two half fibers from neighboring basal bodies. If there is no neighboring basal body, as is the typical case in *vfl-3*, a half-length distal fiber phenotype should result. Apparent half distal fibers have in fact been observed many times in *vfl-3* sections (for example Figs. 2*e* and 4*f*). The model also predicts that the banding pattern of the complete distal fiber should show apparent mirror-image symmetry about its midline, as it indeed does.

Unlike the single distal fiber, each of the two shorter proximal fibers does not connect geometrically equivalent sites on the two basal bodies. Here it can be imagined that one site serves to initiate fiber assembly and the other site serves to receive a fiber initiated from its partner basal body. This model predicts that proximal fibers will to grow to full length on solitary basal bodies, and this does appear to be the case in *vfl-3* (for example Fig. 4*b* and *c*). Furthermore, if proximal fiber assembly originates at only one of the two attachment sites on each basal body, an unpaired basal body should never carry two proximal fibers; this, too, has proved to be the rule.

FIGURE 5 Abnormal rootlet microtubule arrangements in *vfl-3*. (*A*) Wild-type section showing the cruciate orientation of the rootlet microtubules which converge between the basal bodies. Both proximal striated fibers are visible as well. Collidine fixation. (*B*) Wild-type section similar to that in *A*. Note the two probasal bodies in their characteristic positions. Collidine fixation. (*C*) *vfl-3* section showing microtubular rootlets oriented parallel to each other rather than coverging between basal bodies. Collidine fixation. (*D*) *vfl-3* section with microtubules criss-crossing near basal body. Electron-dense material of unknown identity appears to be associated with the microtubules. Collidine fixation. (*E*) Apparently normal microtubular rootlet associated with a solitary *vfl-3* basal body. Collidine fixation. (*F*) *vfl-3* section showing three mature basal bodies in cross section. Note microtubules criss-crossing between one basal-body pair, and an incomplete distal fiber pointing from one basal body towards the other. The third basal body appears free of rootlet associations, but possesses a striated projection. One probasal body is in a normal position relative to the basal-body pair and associated rootlet microtubules, but the other two show no evidence of association with rootlets, mature basal bodies or each other. Collidine fixation. (*b*) Basal body. (*p*) Probasal body. (*pf*) Proximal fiber. Bar, 500 nm. × 48,000.

Comparison to Other Mutants

We recently described a variable flagellar number mutation in the gene *vfl-2* (19). The *vfl-3* and *vfl-2* phenotypes differ in several significant respects. (*a*) Cell size is normal in *vfl-2*. (*b*) Striated fibers of normal morphology are present in many *vfl-2* cells (our unpublished micrographs). (*c*) Extra basal bodies are not present in *vfl-2*. It is thus clear that not all variable flagellar number mutants have striated fiber or cell division defects. Analysis of additional mutants should reveal whether or not such defects are rare or common features of the *vfl* phenotype.

The variable flagellar number mutant *cyt-1* which was described by Warr (41) is also quite different in phenotype from *vfl-3*. *cyt-1* cells are large, multi-lobed, and genrally multinucleate. The *cyt-1* flagella exist in pairs, usually with one pair for each nucleus. The defect in *cyt-1* appears to concern the completion of cytokinesis, and there is no reason to expect it to have striated fiber defects.

There exists a mutant of the multicellular alga *Volvox carteri* which resembles *vfl-3* in a number of respects. In this mutant, S-16 (25), cells divide abnormally to yield progeny of unequal size and of improper orientation with respect to the organism as a whole. As an apparent consequence of its defect in cytokinesis, embryogenesis in S-16 is grossly aberrant. Like *vfl-3*, cells of the mutant show a variable flagellar number phenotype (D. Kirk, personal communication).

Inferences about Striated Fiber Function

Because striated fibers are incomplete or absent in *vfl-3*, we can rule out an essential role for complete fibers in all functions which *vfl-3* cells perform correctly. We therefore conclude that complete fibers are *not* required: (*a*) for the backward swimming response, (*b*) for mating, (*c*) to anchor the basal bodies in the cytoplasm so that they are not torn out by the force of flagellar beating, and (*d*) to maintain equality of flagellar length in multiply flagellated cells.

Vfl-3 is clearly defective in regulation of flagellar number, proper placement of basal bodies in the cell, the establishment or maintenance of proper spatial orientation of flagellar wave forms, and accurate partitioning of the cytoplasm at cytokinesis. Striated fibers could be essential to any or all of these phenomena; alternatively, the *vfl-3* phenotype could represent a defect in an underlying cellular organizing system about which we are not aware. However, an indirect argument, based on our failure to see complete fibers in *vfl-3* sections, does suggest a primary defect in fiber assembly. In 1975 Goodenough and St. Clair (9) reported that in the basal-body defective mutant *bald-2* complete distal fibers unattached to basal bodies were present in the basal-body region of the cell. Since *bald-2* cells have only very rudimentary basal bodies their result suggests that complete fiber assembly can occur without basal bodies. If complete fibers can assemble independent of the basal bodies, it becomes difficult to explain the absence of complete fibers in *vfl-3* on the basis of a defect in basal-body structure or placement, making the possibility of a primary defect in fiber assembly more attractive.

Support for this work was provided by grants PCM-7823253 and PCM-8119065 from the National Science Foundation. J. W. Jarvik was the recipient of Research Career Development Award K04 AM00710 from the National Institutes of Health.

Received for publication 18 August 1982, and in revised form 22 February 1983.

Note Added in Proof: We have examined eight additional *vfl* mutants and observed apparently normal striated fibers in each. Thus a gross fiber-defective phenotype is not typical of *vfl* mutants as a class.

REFERENCES

1. Allen, R. D. 1969. The morphogenesis of basal bodies and accessory structures of the cortex of the ciliated protozoan *Tetrahymena pyriformis*. *J. Cell Biol.* 40:716–733.
2. Anderson, R. G. W. 1977. Biochemical and cytochemical evidence for ATPase activity in basal bodies isolated from oviduct. *J. Cell. Biol.* 74:547–560.
3. Brown, D. L., A. Massalski, and R. Patenaude. 1976. Organization of the flagellar apparatus and associated microtubules in the quadriflagellate alga *Polytomella agilis*. *J. Cell Biol.* 69:106–125.
4. Cavalier-Smith, T. 1974. Basal body and flagellar development during the vegetative cell cycle and the sexual cycle of *Chlamydomonas reinhardtii*. *J. Cell Sci.* 16:529–556.
5. Dingle, A. D., and D. E. Larson. 1981. Structure and protein composition of the striated flagellar rootlets of some protists. *Biosystems.* 14:345–358.
6. Fawcett, D. W., and K. R. Porter. 1954. A study of the fine structures of ciliated epithelia. *J. Morphol.* 94:221–282.
7. Frisch, D., and E. J. Reith. 1966. An interbasal body apparatus in mammalian cells. *J. Ultrastruct. Res.* 15:490–495.
8. Gardiner, P. R., and M. C. P. Marsh. 1977. Studies of a protozoan rootlet—the rhizoplast of *Naegleria*. *J. Protozool.* 24:46*a*. (Abstr.)
9. Goodenough, W. W., and H. S. St. Clair. 1975. Bald-2: a mutation affecting the formation of doublet nd triplet sets of microtubules in *Chlamydomonas reinhardtii*. *J. Cell Biol.* 66:480–491.
10. Goodenough, W. W., and Weiss, R. L. 1976. Interrelationships between microtubules, a striated fiber, and the gametic mating structure of *Chlamydomonas reinhardtii*. *J. Cell Biol.* 76:430–438.
11. Gould, R. R. 1975. The basal bodies of *Chlamydomonas reinhardtii*. *J. Cell Biol.* 65:65–74.
12. Hoffman, L. R. 1970. Observation on the fine structure of *Oedogonium*. IV. The striated component of the compound flagellar roots of *O. cardiacum*. *Can. J. Bot.* 48:189–196.
13. Huang, B., Z. Ramanis, S. K. Dutcher, and D. J. L. Luck. 1982. Uniflagellar mutants of *Chlamydomonas*: evidence for the role of basal bodies in transmission of positional information. *Cell.* 29:745–753.
14. Hufnagle, L. A. 1969. Cortical ultrastructure of *Paramecium aurelia*. *J. Cell Biol.* 40:779–801.
15. Hyams, J. S., and G. G. Borisy. 1975. Flagellar coordination in *Chlamydomonas reinhardtii*. *Science (Wash. DC).* 189:891–893.
16. Jarvik, J. W., and J. L. Rosenbaum. 1980. Oversized flagellar membrane protein in paralyzed mutants of *Chlamydomonas reinhardtii*. *J. Cell Biol.* 85:258–272.
17. Johnson, U. W., and K. R. Porter. 1968. Fine structure of cell division in *Chlamydomonas reinhardtii*. *J. Cell Biol.* 38:403–425.
18. Kates, J. R., and R. F. Jones. 1964. The control of gametic differentiation in liquid cultures of *Chlamydomonas*. *J. Cell. Comp. Physiol.* 63:157–164.
19. Kuchka, M. R., and J. W. Jarvik. 1982. Analysis of flagellar size control using a mutant of *Chlamydomonas reinhardtii* with a variable number of flagella. *J. Cell Biol.* 92:170–175.
20. Larson, D. E., and A. D. Dingle. 1981. Isolation, ultrastructure, and protein composition of the flagellar rootlet of *Naegleria gruberi*. *J. Cell Biol.* 89:424–432.
21. Lauweryns, J. M., and L. Boussaw. 1972. Centrioles and associated striated filamentous bundles in rabbit pulmonary lymphatic endothelial cells. *Z. Zellforsch. Mikrosk. Anat.* 131:417–430.
22. Levine, R. P., and W. T. Ebersold. 1960. The genetics and cytology of *Chlamydomonas*. *Annu. Rev. Microbiol.* 14:197–216.
23. Lewin, R. A. 1952. Ultraviolet induced mutations in *Chlamydomonas moeuwsii gerloff*. *J. Gen. Microbiol.* 11:358–369.
24. Matsusaka, T. 1967. ATPase activity in the ciliary rootlet of human retinal rods. *J. Cell Biol.* 33:203–208.
25. Mattson, D. M., J. L. Bryant, K. J. Green, and D. L. Kirk. 1982. Genetic lesions of cytoskeleton mediated morphogenesis in *Volvox*. *J. Cell Biol.* 95:(2, Pt. 2):353*a*. (Abstr.)
26. Melkonian, M. 1980. Ultrastructural aspects of basal body associated fibrous structures in green algae: a critical review. *Biosystems.* 12:38–104.
27. Moestrup, O. 1978. On the phylogenetic validity of the flagellar apparatus in green algae and chlorophyll *a* and *b* containing plants. *Biosystems.* 10:117–144.
28. Olsson, R. 1962. The relationship between ciliary rootlets and other cell structures. *J. Cell Biol.* 15:596–599.
29. Perkins, D. D. 1952. The detection of linkage in tetrad analysis. *Genetics.* 38:187–197.
30. Pitelka, D. R. 1974. Basal bodies and root structures. *In* Cilia and Flagella. M. A. Sleigh, editor. Academic Press, Inc., New York. 437–469.
31. Reynolds E. S. 1963. The use of lead citrate at high pH as an electron-opaque stain in electron microscopy. *J. Cell Biol.* 17:208–212.
32. Ringo, D. D. 1967. Flagellar motion and fine structure of the flagellar apparatus in *Chlamydomonas*. *J. Cell Biol.* 33:543–571.
33. Sager, R., and S. Granick. 1953. Nutritional studies with *Chlamydomonas reinhardtii*. *Ann. NY Acad. Sci.* 56:831–838.
34. Sakaguchi, H. 1965. Pericentriolar filamentous bodies. *J. Ultrastruct. Res.* 12:13–21.
35. Salisbury, J. L., and G. L. Floyd. 1978. Calcium-induced contraction of the rhizoplast of a quadriflagellate green alga. *Science (Wash. DC).* 202:975–977.
36. Simpson, P. A., and A. D. Dingle. 1971. Variable periodicity in the rhizoplast of *Naegleria* flagellates. *J. Cell Biol.* 51:323–327.
37. Sleigh, M. A. 1979. Contractility of the roots of flagella and cilia. *Nature (Lond.).* 277:263–264.
38. Snell, W. J., W. L. Dentler, L. T. Haimo, L. I. Binder, and J. L. Rosenbaum. 1974. Assembly of chick brain tubulin onto isolated basal bodies of *Chlamydomonas reinhardtii*. *Science (Wash. DC).* 185:357–359.
39. Szollosi, D. 1964. The structure and function of centrioles and their satellites in the jellyfish, *Phialidium gregarium*. *J. Cell Biol.* 21:465–479.
40. von Boletzky, S. 1973. Association of mitochondria with ciliary rootlets in squid embryos. *Cytobiologies.* 8:164–167.

41. Warr, J. R. 1968. A mutant of *Chlamydomonas reinhardii* with abnormal cell division. *J. Gen. Microbiol.* 52:243–251.
42. Welsch, U., and V. Storch. 1969. Fine structure and histochemistry of the pharynx and hepatic caecum of *Branchiostoma lanceolatum* (Pallas). *Z. Zellforsch. Mikrock. Anat.* 1020:432.
43. Witman, G. B., K. Carlson, J. Berliner, and J. L. Rosenbaum. 1972. *Chlamydomonas* flagella. I. Isolation and electrophoretic analysis of microtubules. matrix, membranes, and mastigonemes. *J. Cell Biol.* 54:507–539.
44. Wolfe, J. 1972. Basal body fine structure and chemistry. *In* Advances in Cell and Molecular Biology. E. J. Dupraw, editor. Academic Press, Inc., New York. 151–192.